VERSION: DECEMBER 24, 2013
Preprint typeset using LaTeX style emulateapj v. 12/16/11

SLAC-PUB-16151

arXiv:1312.6462v1 [astro-ph.CO] 23 Dec 2013

UPPER BOUND ON THE FIRST STAR FORMATION HISTORY

YOSHIYUKI INOUE[1], YASUYUKI T. TANAKA[2], GRZEGORZ M. MADEJSKI[1] & ALBERTO DOMÍNGUEZ[3]
[1]Kavli Institute for Particle Astrophysics and Cosmology, Department of Physics, Stanford University and SLAC National Accelerator Laboratory, 2575 Sand Hill Road, Menlo Park, CA 94025, USA
[2] Hiroshima Astrophysical Science Center, Hiroshima University, 1-3-1 Kagamiyama, Higashi-Hiroshima, Hiroshima 739-8526, Japan and
[3]Department of Physics & Astronomy, University of California, Riverside, CA 92521, USA

Version: December 24, 2013

ABSTRACT

Our understanding of the nature of the extragalactic background light (EBL) has improved with the recent development of gamma-ray observation techniques. An open subject in the context of the EBL is the reionization epoch, which is an important probe of the formation history of first stars, the so-called Population III (Pop III) stars. Although the mechanisms for the formation of Pop III stars are rather well understood on theoretical grounds, their formation history is still veiled in mystery because of their faintness. To shed light into this matter, we study jointly the gamma-ray opacity of distant objects and the reionization constraints from studies of intergalactic gas. By combining these studies, we obtain a sensitive upper bound on the Pop III star formation rate density as $\dot{\rho}_*(z) < 0.01[(1+z)/(1+7.0)]^{3.4}(f_{\rm esc}/0.2)^{-1}(C/3.0)$ M$_\odot$ yr^{-1} Mpc^{-3} at $z \geq 7$, where $f_{\rm esc}$ and C are the escape fraction of ionizing photons from galaxies and the clumping factor of the intergalactic hydrogen gas. This limit is a ~ 10 times tighter constraint compared with previous studies that take into account gamma-ray opacity constraints only. Even if we do not include the current gamma-ray constraints, the results do not change. This is because the detected gamma-ray sources are still at $z \leq 4.35$ where the reionization has already finished.

Subject headings: stars: Population III – cosmology: dark ages, reionization, first stars – cosmology: diffuse radiation – gamma rays: general

1. INTRODUCTION

First stars, the so-called Population III (Pop III) stars, are believed to have played an important role in the early cosmic evolution by emitting intense radiation and by dispersing heavy elements into the interstellar medium (e.g. Bromm et al. 2009). The formation process of Pop III stars has been theoretically studied in detail. Pop III stars were formed when the Universe was less than a few hundred million years old (e.g. Abel et al. 2002) and their typical mass was $\sim 20-40\ M_\odot$ (Hosokawa et al. 2011, 2012)[1]. However, the star formation history of Pop III stars is highly uncertain. The theoretically predicted peak of the star formation rate of Pop III stars varies by four orders of magnitude, over $\sim 10^{-5}-10^{-1}\ M_\odot$ yr^{-1} Mpc^{-3} (e.g. Bromm & Loeb 2006; Tornatore et al. 2007; Johnson et al. 2008; Trenti & Stiavelli 2009; de Souza et al. 2011). Observationally, it is difficult to directly investigate Pop III stars with current telescopes because Pop III stars are formed at the early stage of the universe's history. Direct measurements will require next generation instruments, as sensitive as the thirty meter telescope[2] and the James Webb Space Telescope[3].

There are various indirect lines of evidence for Pop III stars – such as reionization (e.g. Totani et al. 2006; Ade et al. 2013). Intense ultraviolet (UV) radiation from Pop III stars was very likely to significantly contribute to the ionization of the intergalactic medium (IGM). Measurements of IGM absorption signatures in the spectra of distant quasars and gamma-ray bursts (GRBs), together with the polarization of the cosmic microwave background (CMB), already prove that the IGM has been reionized between redshift $z \sim 6$ and ~ 30 (e.g. Mesinger 2010; Pritchard et al. 2010; Ade et al. 2013).

The Infrared Telescope in Space (*IRTS*) reported an excess in the NIR background, which can be explained by redshifted light from Pop III stars (Matsumoto et al. 2005, see also Tsumura et al. (2013)). However, the required ionizing photon budget to explain this NIR excess would overproduce the measured Thomson scattering optical depth (Madau & Silk 2005). Later it was also found that this excess would be inconsistent with TeV observations of nearby blazars (e.g. Aharonian et. al. 2006, but see also Essey & Kusenko 2010).

Gamma rays propagating through the universe are attenuated by pair production interactions with low-energy photons of the extragalactic background light (EBL; e.g. Gould & Schréder 1966; Jelley 1966; Dwek & Krennrich 2013). We can probe the EBL by measuring the attenuation features in the spectra of distant gamma-ray sources (e.g. Aharonian et al. 2006; Ackermann et al. 2012b; Abramowski et al. 2013; Domínguez et al. 2013). UV radiation fields causing the reionization may induce significant gamma-ray absorption above a few tens of GeV (Oh 2001; Inoue et al. 2010, 2013b).

Based on a galaxy formation model that reproduces the reionization history, it has been shown that it is difficult to distinguish the contribution of Pop III stars through gamma-ray absorption (e.g. Inoue et al. 2013b). On the other hand, without addressing the implications for reionization, Pop III star formation rate density has been constrained through gamma-ray absorption (Raue et al. 2009; Gilmore 2012) or the NIR background (Fernandez & Komatsu 2006). Shull & Venkatesan (2008) have investigated the allowed range of Pop III star formation efficiency using the constraints

E-mail: yinoue@slac.stanford.edu

[1] Pop III stars are divided into Pop III.1 and III.2 (Bromm et al. 2009). Pop III.1 stars are stars formed from cosmological initial conditions, and Pop III.2 stars are zero-metallicity stars but formed from a gas influenced by earlier stars. For simplicity, we treat them as one population.

[2] `http://www.tmt.org`

[3] `http://www.jwst.nasa.gov`

This material is based upon work supported by the U.S. Department of Energy, Office of Science, Office of Basic Energy Sciences, under Contract No. DE-AC02-76SF00515 and NASA.

from the Thomson scattering optical depth, although it depends on the optical depth of IGM after the reionization.

In this Letter, we present new constraints on the Pop III star formation history, jointly taking account of (1): the Thomson scattering optical depth, (2): neutral fraction of IGM, and (3): observed gamma-ray opacity. Since the NIR background measurement is hampered by uncertain intensity of the zodiacal light, we do not include those constraints. Throughout this Letter, we adopt the standard cosmological parameters of $(h, \Omega_M, \Omega_\Lambda) = (0.7, 0.3, 0.7)$.

2. CONSTRAINTS ON FIRST STAR FORMATION HISTORY

Once the star formation history and spectrum of Pop III stars are given, we can derive the Thomson scattering optical depth, neutral fraction, and gamma-ray opacity (see Inoue et al. 2013b, and references therein). Theoretically, the Pop III star formation history $\dot{\rho}_*(z)$ has been extensively studied (e.g. Bromm & Loeb 2006; Tornatore et al. 2007; Johnson et al. 2008; Trenti & Stiavelli 2009; de Souza et al. 2011). Although all models expect the peak of the Pop III star formation history at $z \gtrsim 6$, the expected history is model dependent. In this Letter, we simply assume the broken power-law shape for the Pop III star formation history at redshift z as

$$\dot{\rho}_*(z) = \dot{\rho}_0 \left[\left(\frac{1+z}{1+z_{\rm peak}} \right)^{\alpha} + \left(\frac{1+z}{1+z_{\rm peak}} \right)^{\beta} \right]^{-1}, \qquad (1)$$

where $\dot{\rho}_0$ gives the normalization in the units of $\mathrm{M_\odot\ yr^{-1}\ Mpc^{-3}}$ and $z_{\rm peak}$ is the redshift where the star formation rate of Pop III stars is maximum. We investigate the allowed parameter space of $(\dot{\rho}_0, z_{\rm peak}, \alpha, \beta)$ by comparing against currently available constraints. Since the reionization has occurred at $z \gtrsim 6$, we set $6 \leq z_{\rm peak} \leq 20$. Even if we set $z_{\rm peak} \gtrsim 20$, the limit on the Pop III star formation history does not change significantly. We also set $3 \leq \alpha \leq 8$ and $-5 \leq \beta \leq 0$ expecting the presence of a peak in the star formation history. If we set a delta function-like star formation history, we can expect higher star formation rate density.

We follow Inoue et al. (2013b) for the calculation of the Thomson scattering optical depth, neutral fraction, and gamma-ray opacity. In this Letter, we summarize the key assumptions adopted by us. The cosmic stellar emissivity at a given frequency ν and redshift z is required to evaluate those values and is given by

$$j(\nu, z) = \int_z^\infty \left| \frac{dt}{dz'} \right| dz' f_{\rm esc} \dot{\rho}_*(z') \varepsilon[(1+z')\nu/(1+z), z', z] \times \exp[-\tau_{\rm IGM}(\nu, z', z)], \qquad (2)$$

where $\varepsilon(\nu, z', z)$ is the intrinsic emissivity at frequency ν at z from stars born at z' in units of $\mathrm{erg\ s^{-1}\ Hz^{-1}\ M_\odot^{-1}}$ given by stellar population synthesis models and $\tau_{\rm IGM}$ is the attenuation opacity in the IGM, respectively. We adopt the IGM opacity of Yoshii & Peterson (1994). $f_{\rm esc}$ is the escape fraction of photons from galaxies with energy above the threshold for ionization of hydrogen. We use stellar population synthesis models that provide the spectral energy distributions with zero metallicity, namely the model of Schaerer (2003). We adopt the Salpeter initial mass function (Salpeter 1955) for the mass range of 1-100 $M_\odot$. Recent radiation-hydrodynamics simulations suggest that the typical mass of Pop III stars is limited to $\lesssim 20-40\ M_\odot$ due to the radiation feedback effects (Hosokawa et al. 2011, 2012). If there are Pop III stars with different initial mass functions, our limit on the Pop III star formation history will change by a factor equal to the ratio of the integrals of the mass functions. We neglect the interstellar dust extinction effect.

A key parameter is $f_{\rm esc}$, which we assume here to be 0.2 at all redshifts (Yajima et al. 2011), unless we note otherwise. Observationally, $f_{\rm esc} \simeq 0.05$–0.3 is reported at $z \sim 3$ (Nestor et al. 2013), but values at $z \geq 4$ have not been measured yet. Ono et al. (2010) have set upper limits of $f_{\rm esc} \lesssim 0.6$ at $z = 5.7$ and $f_{\rm esc} \lesssim 0.9$ at $z = 6.6$ for LAEs. Gong & Cooray (2013) independently constrained $f_{\rm esc}$ as ~ 0.5 at $z = 3$ and ~ 0.9 at $z = 6$ using constraints on gamma-ray opacity. Another key parameter to evaluate the reionization is the clumping factor $C = \langle n_H^2 \rangle / \bar{n}_H^2$, where $n_{\rm H}$ is the hydrogen density (see Inoue et al. 2013b, for details). At $z \gtrsim 6$, C is constrained as $\lesssim 3$ by combining hydrodynamical simulations and the measurements of the Lyα forests (Bolton & Haehnelt 2007). We take $C = 3.0$ as the fiducial value of the parameter unless otherwise noted.

2.1. *Constraint from the Thomson scattering optical depth*

During the reionization epoch, a large population of free electrons is generated in the IGM. Those electrons scatter the CMB photons, and their optical depth can be estimated from the CMB measurements. The measured electron Thomson scattering optical depth τ_e is $\tau_e = 0.092 \pm 0.013$ inferred by the *Planck* data (Ade et al. 2013). Since Population I and II stars also contribute to the reionization, our model must not overproduce the free electron content solely with Pop III stars.

2.2. *Constraint from the neutral fraction of hydrogen*

As the universe was being reionized, the neutral fraction of intergalactic hydrogen $x_{\rm HI}$ also changed. $x_{\rm HI}$ is a good tracer of the ionizing photon production history during the reionization epoch. The discovery of broad troughs of Lyα absorption, the so-called Gunn-Peterson troughs (Gunn & Peterson 1965), in the spectra of distant objects have enabled an estimate of the neutral fraction as $x_{\rm HI} \geq 0.033$ at $z = 6.2$ (Mesinger & Haiman 2007), $x_{\rm HI} \geq 0.1$ at $z = 7.08$ (Mortlock et al. 2011), and $x_{\rm HI} \leq 0.17$ at $z = 6.3$ (Totani et al. 2006).

More ionizing photons and lower neutral fraction are expected, if we take into account the Population I and II stars. Therefore, we constrain the Pop III star formation history not to be less than the lower limit of the neutral fraction. We have not attempted a detailed comparison with Gunn-Peterson measurements of quasars at $z \lesssim 6$. Such effects depend rather sensitively on the dense region of the IGM gas, which is not essential for studying the Pop III star formation at $z \gtrsim 6$.

2.3. *Constraint from the gamma-ray attenuation*

Sufficient UV radiation fields causing cosmic reionization may induce gamma-ray absorption above a few tens of GeV (Oh 2001; Inoue et al. 2010, 2013b). To constrain the gamma-ray opacity at high redshifts, we use the *Fermi*-LAT detected distant sources with detected > 10 GeV photons. Since gamma-ray opacity for photons with ~ 20–70 GeV is close to unity at $z \gtrsim 2$ (e.g. Domínguez et al. 2011; Inoue et al. 2013b), we focus on sources at $z \geq 2$.

Known distant gamma-ray emitting populations are GRBs and blazars. LAT has detected 35 GRBs (Ackermann et al. 2013). Since more distant sources can put tighter constraints on the Pop III star formation rate, we use the most distant one GRB 080916C at $z = 4.35$, which had photons up

to 13.22 GeV. We select blazars having Test Statistics (TS) > 100, photon index $\Gamma \leq 2.0$, and $z > 2.0$ from the second catalog of *Fermi*-LAT sources (2FGL Nolan et al. 2012). After the selection, flat spectrum radio quasar 2FGL J1344-1723 at $z = 2.506$ survives with TS=967.

For both the GRB and blazar cases, we reduced *Fermi*-LAT data and performed an unbinned maximum likelihood analysis using Fermi Science Tool version v9r27p1. For 2FGL J1344-1723, the analyzed time interval is MET 239557417 (2008-08-04 15:43:36 UT) to 386632050 (2013-04-02 21:47:27 UT) representing a total of $\sim$4.7 years of data. For GRB 080916C, we used the first 1000 seconds after the burst [4] (MET 243216766–243217766). We extracted 0.1–300 GeV `SOURCE` class events within 10° circles centered at the source positions. Good time intervals were generated using the recommended filter of `(DATA_QUAL==1)&&(LAT_CONFIG==1)&&ABS(ROCK_ANGLE)<52` and an ROI-based zenith angle cut (`roicut=yes`) with a maximum zenith angle cut of 100°. We utilized `P7SOURCE_V6` as the Instrument Response Functions. In the source model of 2FGL J1344-1723, we modeled the spectrum as a log-parabola and included all the 2FGL sources within a 10° circle. The spectral parameters of these sources were left free in the likelihood fitting. 2FGL sources within an annulus of 10° to 15° from the source were also included in the model, but their spectral parameters were fixed to the 2FGL values. In the source model of GRB 080916C, we included only this burst by modeling its spectrum with a single power-law function. Galactic and extragalactic diffuse emissions were modeled with the recommended template files (`gal_2yearp7v6_v0.fits` and `iso_p7v6source.txt`), where the normalizations of both components were set free and the standard power-law scaling was applied to the Galactic one. As a result, we obtained a photon index of $\alpha = 2.08 \pm 0.06$ and a curvature parameter $\beta = 0.10 \pm 0.03$ for 2FGL J1344-1723 and $\Gamma = 2.18 \pm 0.08$ for GRB 080916C. To construct the LAT spectrum, we divided the whole energy range into bins defined by energies of 0.1–0.3, 0.3–1.0, 1.0–3.0, 3–10, 10–30, and 30–100 GeV and performed a maximum-likelihood analysis using `gtlike` in each energy bin. We assumed single power-law shapes for both sources allowing the normalization to vary. Here the power law index was fixed to the values obtained by `gtlike` from the whole energy-range (0.1–300 GeV) data set for GRB 080916C, while we utilize the α value of the log-parabola spectrum for 2FGL J1344-1723. For the surrounding sources and the two (Galactic and isotropic) diffuse components, the spectral parameters were again fixed to the values obtained by `gtlike` for the whole energy range and only the normalizations were left free. The estimated systematic uncertainty on the γ-ray flux is 10% at 100 MeV, decreasing to 5% at 560 MeV, and increasing to 10% at 10 GeV and above (Ackermann et al. 2012a).

To constrain the gamma-ray opacity, an intrinsic spectrum is required. There are various models to explain blazar and GRB spectra. We follow general arguments based on the shock acceleration scenario. First-order Fermi acceleration is the broadly accepted model, and the resulting particle spectrum is expected to show a power-law shape of $dN/dE \propto E^{-p}$ with a slope $p \sim 2$. The slope p can be steeper than 2 due to cooling effects. The expected photon index from the inverse Compton scattering radiation by electrons will be $\Gamma \geq (1+p)/2$, while that from hadronic processes will be $\Gamma = p$, where the photon spectrum is given by $dN_{\gamma}/dE \propto E^{-\Gamma}$. The resulting photon index of the intrinsic spectrum is $\Gamma \geq 1.5$ (e.g. Aharonian et al. 2006). If we assume a softer intrinsic spectrum, we can obtain a tighter constraint on Pop III star formation rate density. To be conservative, we take $\Gamma = 1.5$ (e.g. Aharonian et al. 2006) from the energy bin of 3.0–10.0 GeV, which is the highest energy bin among the data points not affected by the gamma-ray attenuation. The gamma-ray opacity at energy E and redshift z is estimated as $\tau_{\gamma\gamma}(E,z) = \ln[F_{\rm int}(E)/F_{\rm obs}(E)]$, where $F_{\rm int}$ is the intrinsic flux and $F_{\rm obs}$ is the observed flux. We take this opacity as an upper limit. Figure 1 shows the derived opacity limit for 2FGL J1344-1723 and GRB 080916C. The derived upper limit at $E = 17.3$ GeV is $\tau_{\gamma\gamma} \leq 2.93$ and ≤ 1.03 at $z = 2.506$ and $z = 4.35$, respectively. We also show the opacity from the model of Inoue et al. (2013b) for reference. We note that hadron-induced gamma rays may appear above several hundred GeV (Essey & Kusenko 2010).

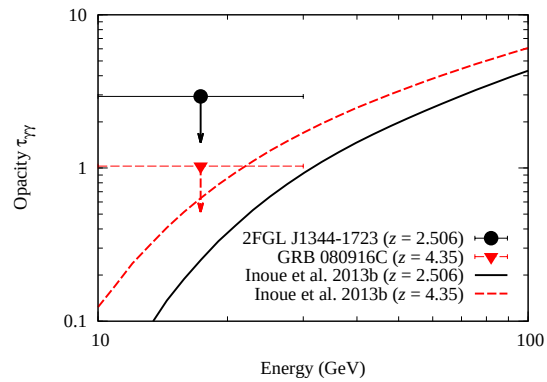

FIG. 1.— Derived upper limits for the optical depth at $z = 2.506$ (2FGL J1344-1723, solid arrow) and, $z = 4.35$ (GRB 080916C, dashed arrow). For the comparison, we also plot an expected optical depth from an EBL model by curves (Inoue et al. 2013b).

In summary, constraints on Pop III stars obtained by current available observations are $\tau_e \leq 0.092$ (Ade et al. 2013), $x_{\rm HI} \geq 0.033$ at $z = 6.2$ (Mesinger & Haiman 2007), $x_{\rm HI} \geq 0.1$ at $z = 7.08$ (Mortlock et al. 2011), $\tau_{\gamma\gamma} \leq 2.93$ at $E = 17.3$ GeV and $z = 2.506$, and $\tau_{\gamma\gamma} \leq 1.03$ at $E = 17.3$ GeV and $z = 4.35$. Since probability functions of these limits are uncertain, we set the upper limits by taking the maximum allowed star formation rate density at each redshift within each allowed parameter spaces. Therefore, first, we estimate τ_e, $x_{\rm HI}$ and $\tau_{\gamma\gamma}$ in all the combinations of parameters. Second, we choose parameter sets that do not violate the given observational constraints. Lastly, we take the maximum of the star formation rate density at each redshift from the allowed parameter sets and set those as the upper limit on the Pop III star formation history.

3. RESULTS

Figure 2 shows the upper limits on the Pop III star formation history. Thick solid, dashed, and dotted curves with arrows show the upper limit on the Pop III star formation rate density for $(C, f_{\rm esc}) = (3.0, 0.2)$, $(3.0, 0.5)$, and $(1.0, 0.2)$, respectively. The upper limit above $z = 7$ can be approximated as

$$\dot{\rho}_*(z) < 0.01 \left[\frac{(1+z)}{(1+7.0)}\right]^{3.4} \left(\frac{f_{\rm esc}}{0.2}\right)^{-1} \left(\frac{C}{3.0}\right) {\rm M}_{\odot}\ {\rm yr}^{-1}\ {\rm Mpc}^{-3}. \quad (3)$$

[4] `http://fermi.gsfc.nasa.gov/ssc/observations/types/grbs/grb_table/`

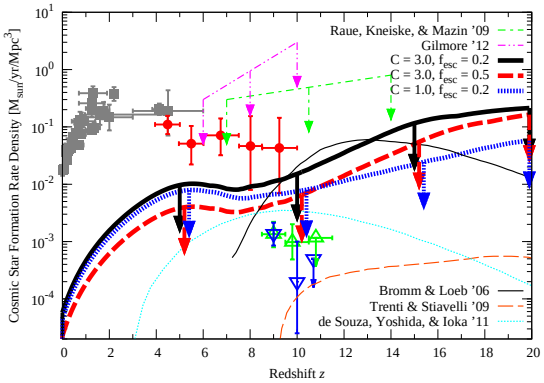

FIG. 2.— Upper limits on the Pop III star formation history. Thick solid, dashed, and dotted curve with arrows represents the upper limit for $(C, f_{\rm esc}) = (3.0, 0.2)$, $(3.0, 0.5)$, and $(1.0, 0.2)$, respectively. For comparison, we show the previously studied upper limits by Raue et al. (2009) and Gilmore (2012) with thin dot-dashed line and double-dot-dashed line with arrows. We plot theoretical models for the Pop III star formation by Bromm & Loeb (2006), thin solid curve; Trenti & Stiavelli (2009) (Pop III.2), dashed curve; and de Souza et al. (2011) (Pop III.2), dot-dashed curve. For de Souza et al. (2011), we adopt their optimistic model. We also plot the observational data compiled by Hopkins (2004, filled square), that deduced from high redshift galaxies (Ellis et al. 2013; Oesch et al. 2013, up-triangle, and down-triangle, respectively), and that inferred from GRBs (Kistler et al. 2013, circle). These data points represent the summation of all stellar populations. For the high redshift galaxies, limiting luminosities are adopted by each author.

For comparison, we show the upper-limits from previous studies (Raue et al. 2009; Gilmore 2012), which do not take into account the reionization constraints. The upper limit becomes 10 times tighter by including the reionization data. The upper limit does not change significantly when we exclude the constraints from the *Fermi*-LAT data. This is because the most distant gamma-ray objects with > 10 GeV photons are still not beyond $z \sim 6$ where the reionization occurred.

We also plot the cosmic star formation rate density data compiled by Hopkins (2004), deduced from distant galaxies (Ellis et al. 2013; Oesch et al. 2013), and inferred from GRBs (Kistler et al. 2013). We note that these data represent all stellar populations. Each high redshift galaxy data point is obtained by integrating its luminosity function down to a limiting luminosity. We note that the overall UV luminosity function at these redshifts is still uncertain due to poor statistics (Ellis et al. 2013; Oesch et al. 2013).

We compare our limits with theoretically studied Pop III star formation rates in the literature, specifically in Bromm & Loeb (2006, Pop III.1 + III.2), Trenti & Stiavelli (2009, Pop III.2), and de Souza et al. (2011, Pop III.2). For de Souza et al. (2011), we take their optimistic model where they assume a very high star formation efficiency and low chemical enrichment. The Pop III star formation model by Bromm & Loeb (2006) violates the current observational constraints.

If remnants of Pop III stars became seeds of supermassive black holes (SMBHs), which would manifest themselves as quasars observed at $z \sim 6$ (e.g. Mortlock et al. 2011), the presence of such quasars may tighten our limits. In this Letter, we do not take into account this constraint because of our poor knowledge of accretion and merger history of such seed BHs, and their precursors. It may be difficult to create SMBHs from Pop III stars because radiation feedback terminates Pop III stars growing above a few tens solar masses (e.g. Hosokawa et al. 2011). Promising candidates for seeds of SMBHs can be formed by a direct collapse of supermassive stars (Hosokawa et al. 2013). Since their effective temperature is less than 10^4 K because of large radius of such supermassive stars, they will not significantly contribute to the reionization.

4. CONCLUSIONS

In this Letter, we show that considering simultaneously the current measurements of gamma-ray opacity, the electron Thomson scattering optical depth, and the neutral fraction set an upper limit of $\dot{\rho}_*(z) < 0.01[(1+z)/(1+7.0)]^{3.4}(f_{\rm esc}/0.2)^{-1}(C/3.0)$ $M_\odot$ yr^{-1} Mpc^{-3} on the Pop III star formation rate density above $z = 7$. By including the reionization constraints, the upper limit becomes ~ 10 times tighter compared to previous works (Raue et al. 2009; Gilmore 2012).

Current gamma-ray data do not strongly constrain the Pop III star formation history because the most distant object is still at $z = 4.35$ where the reionization process is completed. To explore the reionization epoch via the gamma-ray technique, sources beyond redshift 6 and rich with > 10 GeV photons would be needed (Inoue et al. 2013b). *Fermi* may eventually detect blazars at $z > 6$ (Inoue et al. 2011), and the Cherenkov Telescope Array may possibly do the same at ~ 30 GeV for GRBs (Inoue et al. 2013a). Tanaka et al. (2013) have reported the detection of >100 GeV photons from a blazar at $z = 1.1$ and Takahashi et al. (2013) have reported a candidate *Fermi* gamma-ray blazar at $z \sim 3-4$. Future gamma-ray observations of distant sources at $\gtrsim 10$ GeV will put tighter constraints on Pop III star formation history by combining reionization measurements.

We acknowledge M. Ajello, J. Chiang, L. Latronico, P. Marshall, J. Perkins, J. Scargle, and D. Thompson for useful comments. The *Fermi*-LAT Collaboration acknowledges support from a number of agencies and institutes for both development and the operation of the LAT as well as scientific data analysis. These include NASA and DOE in the United States, CEA/Irfu and IN2P3/CNRS in France, ASI and INFN in Italy, MEXT, KEK, and JAXA in Japan, and the K. A. Wallenberg Foundation, the Swedish Research Council and the National Space Board in Sweden. Additional support from INAF in Italy and CNES in France for science analysis during the operations phase is also gratefully acknowledged.

REFERENCES

Abel, T., Bryan, G. L., & Norman, M. L. 2002, Science, 295, 93
Abramowski, A. et al. 2013, A&A, 550, A4
Ackermann, M. et al. 2012a, ApJS, 203, 4
—. 2012b, Science, 338, 1190
—. 2013, arXiv:1303.2908
Ade, P. A. R. et al. 2013, arXiv:1303.5076
Aharonian, F. et al. 2006, Nature, 440, 1018
Bolton, J. S. & Haehnelt, M. G. 2007, MNRAS, 382, 325
Bromm, V. & Loeb, A. 2006, ApJ, 642, 382
Bromm, V., Yoshida, N., Hernquist, L., & McKee, C. F. 2009, Nature, 459, 49
de Souza, R. S., Yoshida, N., & Ioka, K. 2011, A&A, 533, A32
Domínguez, A., Finke, J. D., Prada, F., Primack, J. R., Kitaura, F. S., Siana, B., & Paneque, D. 2013, ApJ, 770, 77
Domínguez, A. et al. 2011, MNRAS, 410, 2556
Dwek, E. & Krennrich, F. 2013, Astroparticle Physics, 43, 112
Ellis, R. S. et al. 2013, ApJ, 763, L7
Essey, W. & Kusenko, A. 2010, Astroparticle Physics, 33, 81

Fernandez, E. R. & Komatsu, E. 2006, ApJ, 646, 703
Gilmore, R. C. 2012, MNRAS, 420, 800
Gong, Y. & Cooray, A. 2013, ApJ, 772, L12
Gould, R. J. & Schréder, G. 1966, Physical Review Letters, 16, 252
Gunn, J. E. & Peterson, B. A. 1965, ApJ, 142, 1633
Hopkins, A. M. 2004, ApJ, 615, 209
Hosokawa, T., Omukai, K., Yoshida, N., & Yorke, H. W. 2011, Science, 334, 1250
Hosokawa, T., Yorke, H. W., Inayoshi, K., Omukai, K., & Yoshida, N. 2013, ApJ, 778, 178
Hosokawa, T., Yoshida, N., Omukai, K., & Yorke, H. W. 2012, ApJ, 760, L37
Inoue, S., Salvaterra, R., Choudhury, T. R., Ferrara, A., Ciardi, B., & Schneider, R. 2010, MNRAS, 404, 1938
Inoue, S. et al. 2013a, Astroparticle Physics, 43, 252
Inoue, Y., Inoue, S., Kobayashi, M. A. R., Makiya, R., Niino, Y., & Totani, T. 2013b, ApJ, 768, 197
Inoue, Y., Inoue, S., Kobayashi, M. A. R., Totani, T., Kataoka, J., & Sato, R. 2011, MNRAS, 411, 464
Jelley, J. V. 1966, Physical Review Letters, 16, 479
Johnson, J. L., Greif, T. H., & Bromm, V. 2008, MNRAS, 388, 26
Kistler, M. D., Yuksel, H., & Hopkins, A. M. 2013, arXiv:1305.1630
Madau, P. & Silk, J. 2005, MNRAS, 359, L37
Matsumoto, T. et al. 2005, ApJ, 626, 31
Mesinger, A. 2010, MNRAS, 407, 1328
Mesinger, A. & Haiman, Z. 2007, ApJ, 660, 923
Mortlock, D. J. et al. 2011, Nature, 474, 616
Nestor, D. B., Shapley, A. E., Kornei, K. A., Steidel, C. C., & Siana, B. 2013, ApJ, 765, 47
Nolan, P. L. et al. 2012, ApJS, 199, 31
Oesch, P. A. et al. 2013, arXiv:1301.6162
Oh, S. P. 2001, ApJ, 553, 25
Ono, Y., Ouchi, M., Shimasaku, K., Dunlop, J., Farrah, D., McLure, R., & Okamura, S. 2010, ApJ, 724, 1524
Pritchard, J. R., Loeb, A., & Wyithe, J. S. B. 2010, MNRAS, 408, 57
Raue, M., Kneiske, T., & Mazin, D. 2009, A&A, 498, 25
Salpeter, E. E. 1955, ApJ, 121, 161
Schaerer, D. 2003, A&A, 397, 527
Shull, J. M. & Venkatesan, A. 2008, ApJ, 685, 1
Takahashi, Y., Kataoka, J., Niinuma, K., Honma, M., Inoue, Y., Totani, T., Inoue, S., Nakamori, T., & Maeda, K. 2013, arXiv:1306.3552
Tanaka, Y. T. et al. 2013, arXiv:1308.0595
Tornatore, L., Ferrara, A., & Schneider, R. 2007, MNRAS, 382, 945
Totani, T., Kawai, N., Kosugi, G., Aoki, K., Yamada, T., Iye, M., Ohta, K., & Hattori, T. 2006, PASJ, 58, 485
Trenti, M. & Stiavelli, M. 2009, ApJ, 694, 879
Tsumura, K., Matsumoto, T., Matsuura, S., Sakon, I., & Wada, T. 2013, arXiv:1307.6740
Yajima, H., Choi, J.-H., & Nagamine, K. 2011, MNRAS, 412, 411
Yoshii, Y. & Peterson, B. A. 1994, ApJ, 436, 551